Life Sciences 239 (2019) 117035

Contents lists available at ScienceDirect

Life Sciences

journal homepage: www.elsevier.com/locate/lifescie

Taurine up-regulated 1 accelerates tumorigenesis of colon cancer by regulating miR-26a-5p/MMP14/p38 MAPK/Hsp27 axis *in vitro* and *in vivo*

Lei Tian[a,*,1], Zhi-Feng Zhao[b,1], Ling Xie[c], Jin-Peng Zhu[a]

[a] Department of Gastroenterol, Jinzhou Medical University, Affilliated Hospital 1, Jinzhou, 121000, Liaoning Province, People's Republic of China
[b] Department of Gastroenterol, the Fourth Affiliated Hospital of China Medical University, Shenyang, 110000, Liaoning Province, People's Republic of China
[c] Department of Anatomy, Jinzhou Medical University, Jinzhou, 121000, Liaoning Province, People's Republic of China

ARTICLE INFO

Keywords:
Colon cancer
Taurine-upregulated gene 1
miR-26a-5p
Metastasis
Oncogenicity

ABSTRACT

Aims: The purpose of this study was to investigate the role of long non-coding RNA taurine-upregulated gene 1 (TUG1) in colon cancer (*Cc*) and related molecular mechanisms.
Materials and methods: RT-qPCR, Western blot and immunohistochemistry were used to detect the expression of related proteins. BrdU and Transwell assays were used to detect cell proliferation and invasion, respectively. Immunofluorescence was used to detect the expression of Vimentin.
Key findings: TUG1 expression was up-regulated in CaCO-2, SW620 and HT-29 cells, while miR-26a-5p was **down**-regulated. Bioinformatics analysis showed that miR-26a-5p was the target of TUG1, and the targeting relationship was further confirmed by dual-luciferase report analysis. Besides, matrix metalloproteinases-14 (MMP-14) was a target of mir-26a-5p. Knockdown of TUG1 by shRNA (sh-TUG1) inhibited MMP-14 expression. Functional analysis showed that sh-TUG1 significantly inhibited *Cc* cell proliferation, invasion and epithelial-mesenchymal transformation (EMT). Notably, miR-26a-5p inhibitor reversed the promotion of *Cc* caused by sh-TUG1. Mechanically, the overexpression of TUG1 significantly up-regulated the levels of MMP-14, VEGF, p-p38 mitogen-activated protein kinase (p-p38 MAPK) and p-HSP27 (heat shock protein 27), and promoted the proliferation, invasion and EMT of *Cc* cells. However, MAPK pathway inhibitor SB203580 has shown the opposite effect. Additionally, animal studies have shown that sh-TUG1 inhibited tumor growth and motility *in vivo* in the same way.
Significance: This study demonstrated that TUG1 accelerates the development of colon cancer by regulating miR-26a-5p/MMP14/p38 MAPK/Hsp27 axis *in vitro* and *in vivo*. Therefore, TUG1 provides a new direction for the treatment of *Cc*.

1. Introduction

Colon cancer (*Cc*) is the third malignant tumor worldwide with no obvious symptoms in the early stage [20]. In China, the incidence of *Cc* is growing at a rate of 3.9% per year. With the development of gastrointestinal endoscopy, the early diagnosis rate of *Cc* has increased [18]. Clinically, cytoreductive surgery combined with chemotherapy was used to treat *Cc* [4]. Although adjuvant therapy has been widely used, the overall survival rate of patients is still very low [1,15]. Therefore, it is of great significance to explore the molecular mechanism of *Cc* for clinical effective treatment.

Taurine-upregulated gene 1 (TUG1) is a novel lncRNA located on chr22q12.2 and upregulated by taurine in retinal cells of mice [26]. Extensive studies have shown that TUG1 is associated with a variety of cancers, including laryngeal cancer [31] and hepatocellular carcinoma [5]. Previous studies have shown that overexpression of TUG1 promoted tumorigenesis of *Cc* [29]. However, the molecular mechanism of TUG1 remains to be further studied.

miR-26a-5p is a tumor suppressor gene that blocks cell cycle and cell proliferation [16]. Numerous studies have shown that miR-26a-5p miR-26a-5p contributed to inhibit the occurrence of various diseases, especially cancers, such as lung adenocarcinoma [19] and bladder cancer [21]. Matrix metalloproteinase-14 (MMP-14) is a transmembrane protein hydrolase that simultaneously degrades cytokines and growth factors [7]. Studies have shown that MMP-14 promoted angiogenesis, invasion and metastasis manily by up-regulating vascular

* Corresponding author. Department of Gastroenterol, the First Affiliated Hospital of Jinzhou Medical University, No.2 Fifth Duan, People Street, Gucheng District, Jinzhou 121000, Liaoning Province, People's Republic of China.
E-mail address: yleitianxq@sina.com (L. Tian).
[1] These authors contributed equally to this work and should be considered co-first authors.

https://doi.org/10.1016/j.lfs.2019.117035
Received 26 August 2019; Received in revised form 12 October 2019; Accepted 28 October 2019
Available online 04 November 2019
0024-3205/

endothelial growth factor (VEGF) and mediating the activation of MMP2 enzyme [22]. In recent years, abnormal expression of MMP-14 has also been found in gastric cancer [24], breast cancer [3] and colorectal cancer [27]. Besides, MMP-14 is regulated by a variety of microRNAs, such as miR-133a [2] and miR-26b [13]. However, the effect of miR-26a-5p/MMP-14 interaction on *Cc* and its related molecular mechanism are unclear.

p38 mitogen-activated protein kinase (p38MAPK) is a key protein activated by various inflammatory mediators and environmental stress and plays an important role in proliferation, differentiation and survival [8]. As a primary substrate of p38 MAPK, heat shock protein 27 (Hsp27) is a downstream protein of MAPK-activated protein kinase-2 (MAPKAPK-2; MK2). Previous studies have shown that the activation of the p38 MAPK pathway is involved in the occurrence of colorectal cancer [10]. However, it is unclear whether the p38MAPK/Hsp27 pathway is involved in *Cc*.

To date, the role of TUG1 and its potential molecular mechanisms are not clear. In the present study, we first provided a direct evidence that TUG1 might be employed as a therapeutic target for *Cc*.

2. Material and methods

2.1. Cells and transfection

Human colon cancer cell lines (SW620, HT-29, CaCo-2) and normal human colon fibroblast (CCD-18Co) were purchased from the Cell Bank of the Chinese Academy of Sciences (Shanghai, China). SW620 and HT-29 cells were maintained in RPMI-1640 medium and McCoy's 5A, respectively. Caco-2 and CCD-18Co cells were cultured in Minimum Essential Media (Global Cell Solutions, Charlottesville, VA, USA). All cells were incubated with 10% fetal bovine serum (FBS, Invitrogen, Grand Island, NY, USA), 50 U/ml penicillin and 50 μg/ml streptomycin (Invitrogen, Grand Island, NY, USA) and grown at 37 °C with 5% CO_2. All transfections were performed using Lipofectamine 2000 reagent (Invitrogen, Grand Island, NY, USA) according to the manufacturer's protocol.

2.2. Reverse transcription quantitative real-time PCR (RT-qPCR)

Total RNA extracted from SW620,HT-29, CaCo-2, CCD-18Co and tumor tissues with TRIzol reagent was reverse-transcribed to cDNA by RevertAid First Strand cDNA Synthesis kit (Invitrogen, Grand Island, NY, USA). RT-qPCR was performed by SYBR-Green PCR Master Mix kit (Takara, Japan) and ABI 7500 Real-Time PCR System (Applied Biosystems, USA). RNA was heated at 42 °C for 60 min and incubated at 72 °C for 15 min to synthesize First Strand cDNA. Thereafter, 1 μl of cDNA was mixed with 10 μl of SYBR® Premix Ex Taq™, and 0.5 μl of the corresponding primers was added, and then nuclease-free water was added to a final volume of 20 μl.The reaction was checked using an ABI-7500 real-time PCR system as follows: 95 °C for 30 s, then 48 cycles at 95 °C for 3 s and 53 °C for 42 s. Fold changes were calculated by equation $2^{-\Delta\Delta Ct}$. All results were repeated three times. The primers of GAPDH were 5′-GTCAGGATCCACTCATCACG-3' (sense) and 5′-GATCG GACTTACGGACTCACATC-3' (antisense); The primers of miR-26a were 5′-CTTCGACGGCATACGAAATGCGCC-3' (sense) and 5′-CCTAGGTAAC CAGTAGCTAGCGC-3' (antisense); The primers of TUG1 were 5′-CCGG TAGGGCCACTAAACGTACG-3' (sense) and 5′-GGCTTAAAAGCCGCCC GCATGCC-3′(antisense). The primers of MMP14 were 5′-TACGTTAAA CGTGGCTGCCAGTAACGG-3' (sense) and 5′-TTAGCGGACTAGCAAAG CTGCACCG -3′(antisense). GAPDH was employed as an internal reference.

2.3. TUG1 knockdown and overexpression

ShRNA specific to TUG1 was obtained from GenePharma (Guangzhou, Guangdong, China). The sequence was as follows: 5′-CCAACGAUUUCGUUCCUUTT-3′. For overexpression, the full length of TUG1 were amplified and integrated into LV-MAX (Invitrogen) to obtained TUG1 overexpressing lentivirus (LV-TUG1). SW620 cells were subsequently infected with lentivirus or transfected with sh-TUG1 using Lipofectamine 2000 reagent (Invitrogen, Guangzhou, China).

2.4. Dual luciferase reporter assay

The target of TUG1 was estimated using miRDB (http://mirdb.org). The 3′UTR fragmentsof TUG1 (wt and mut) were amplified and integrated into a luciferase reporter vector (pmirGLO; Promega, USA). Recombinant vectors (Luc-TUG1-wt or Luc-TUG1-mut) or/and miR-26a mimic were transfected into SW620 cells using Lipofectamine 2000 transfection reagent (Invitrogen, Grand Island, NY, USA). Luciferase activity was identified by a dual-luciferase reporter assay kit (Promega, Madison, USA).

2.5. Western blot analysis

SW620 cells and tumor tissue were ground in liquid nitrogen and cleaved in a lysate buffer (Beyotime, Shanghai, China). The proteins was isolated with 8% SDS polyacrylamide gel and transferred to polyvinylidene difluoride (PVDF) membrane (Millipore, IPFL00010, Billerica, MA). After incubation with primary antibodies, the samples were reacted with anti-rabbit IgG (H + L) secondary antibody (#14708, 1:1000, Cell Signaling Technology, Massachusetts, USA) and detected with an enhanced chemiluminescence (ECL) substrate kit (Amersham Biosciences, USA). The primary antibodies MMP-14 (#13130, 1:1000), E-cadherin (#3195, 1:1000), Vimentin (#5741, 1:1000), N-cadherin (#13116, 1:1000), VEGF (#9698, 1:1000), p38 (#8690, 1:1000), p-p38 (#4511, 1:1000), HSP27 (#95357, 1:1000), p-HSP27 (#9709, 1:1000) and GAPDH (#5174, 1:1000) were all from Cell Signaling Technology (Massachusetts, USA). Relative protein levels was tested by ImageJ software. The experiments were repeated independently in triplicate.

2.6. BrdU staining assay

The transfected SW620 cells were inoculated in 96-well plates and cultured overnight. BrdU (10 μg/mL) was added to the medium and incubated for another 1 h. The cells were then fixed in 4% paraformaldehyde for 10 min and stained with anti-BrdU antibody (Biocompare, South San Francisco, CA) according to the manufacturer's instructions. Finally, the cells were counterstained with DAPI and photographed with fluorescence microscopy (Olympus, Tokyo, Japan). The experiments were repeated independently in triplicate.

2.7. Transwell assay

Transwell assay was employed to measure the invasive capacity of SW620 cells. Matrigel was diluted with serum-free DMEM medium, coated on the surface of the upper chamber and dried at room temperature. Cells were starved in serum-free medium for 24 h, and cell suspension was collected and transferred to the upper chambers (200 ml per chamber). The lower chamber was added with 600 μl medium containing 10% FBS. After 48 h of culture at 37 °C, the upper chamber was removed and washed with PBS. Wipe off the residual cells on the upper membranes with a cotton bud. The cells in the lower chamber were then fixed with 95% alcohol, stained with crystal violet and observed under a microscope (Leica, Germany). The experiments were repeated independently in triplicate.

2.8. Animal models

All animal experiments were carried out in accordance with the NIH Guide for the Care and Use of Laboratory Animals and were approved

by Jinzhou Medical University. A total of 60 BALB/c nude mice (male, 4-week old) were obtained from the Animal Center of Jinzhou Medical University. The mice were housed in a controlled environment at a temperature of 25 ± 3° C and a humidity of 60%, and were housed under a 12-h light/dark cycle with free access to food and water. Untreated SW620 cells or SW620 cells transfected with sh-TUG1 were injected subcutaneously into the flank area of mice. After successful modeling, mice were randomly divided into two groups with ten in each group: Control group and sh-TUG1 group (SW620 cells with sh-TUG1 were injected into mice). After 30 days injection, mice were euthanized by intraperitoneal injection of pentobarbital sodium (200 mg/kg body weight). Tumors were harvested and tumor weight was measured. All experiments were conducted in triplicate.

2.9. Immunofluorescent assay

Immunofluorescence assay was used to estimate changes in vimentin levels in SW620 cells. Briefly, transfected SW620 cells were fixed with 4% paraformaldehyde for 30 min, permeabilized with 0.5% TritonX-100 for another 30 min and then blocked with TBST (containing 5% bovine serum albumin, BSA, Affymetrix, Cleveland, OH) at 37 °C overnight. After pretreatment with primary antibodies against Vimentin (#5741, 1:100, CST) overnight at 4 °C, cells were incubated with Alexa Fluor® 647 Conjugate secondary antibody (#4414, 1:1000, CST), stained with DAPI (1:1000, cat. No. D9564, Sigma-Aldrich) and examined by confocal microscopy (LSM 510 Meta, Zeiss, Oberkochen, Germany). Vimentin spots were counted from more than 10 microscopic fields. The microscopic images were processed as previously described (Cao et al., 2017). The experiments were repeated independently in triplicate.

2.10. Immunohistochemistry (IHC)

IHC was carried out according to the previous methods [12]. Briefly, paraffin sections were deparaffinized in xylene and rehydrated in ethanol at several different gradients. After that, the tissue slices were incubated in 30% H_2O_2 for 30 min to inactivate endogenous peroxidase, and incubated with primary antibodies Ki-67 (#9027, 1:400, CST) and VEGF (#2479, 1:600, CST) at 4 °C overnight. After washing with TBST for three times, the sections were incubated with Alexa Fluor® 488 secondary antibody (Cat # A-21206, 1:500, Thermo Fisher) at room temperature for 3 h. The image was recorded under an optical microscope. The experiments were repeated independently in triplicate.

2.11. Statistical analysis

The statistical analysis was undertaken with SPSS 21.0 (SPSS, Inc, Chicago, IL, USA). Measurement data were presented as mean ± SD (x ± s). Statistical significance was obtained by using Student's *t*-test (both groups) or ANOVA (> 2 group). $*p < 0.05$ were deemed to statistically significant.

3. Results

3.1. The expression of TUG1 was upregulated, while the expression of miR-26a-5p was downregulated in human colon cancer cells

We firstly detected the levels of TUG1 and miR-26a-5p in three colon cancer cell lines (SW620,HT-29 and CaCo-2) and normal human colon fibroblast (CCD-18Co) by RT-qPCR. As shown in Fig. 1A, TUG1 level in SW620,HT-29, CaCo-2 was significantly increased and miR-26a-5p level was significantly decreased compared to CCD-18Co (Fig. 1B). Compared with CCD-18Co, SW620 cell line showed great differences in both TUG1 and miR-26a-5p. Thus, the SW620 cell line was used for subsequent experiments. Taken together, these results demonstrated that TUG1 and miR-26a-5p may be correlated with human colon cancer.

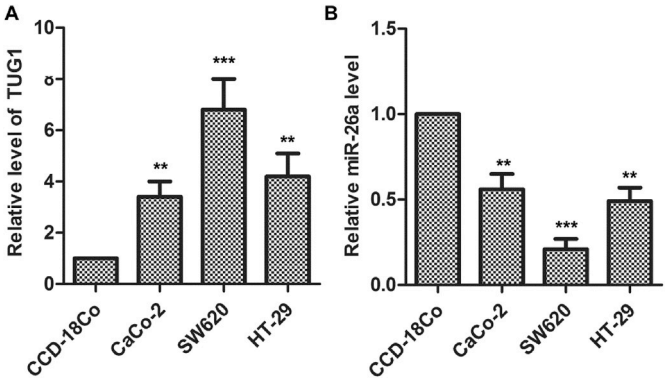

Fig. 1. The expression of TUG1 was upregulated, while the expression of miR-26a-5p was downregulated in human colon cancer cells TUG1 and miR-26a-5p were monitored by RT-qPCR. A. The expression level of TUG1 in three human colon cancer cell lines (SW620,HT-29, CaCo-2) and normal human colon fibroblast (CCD-18Co) was detected by RT-qPCR, B. The expression level of miR-26a-5p in three human colon cancer cell lines (SW620,HT-29, CaCo-2) and normal human colon fibroblast (CCD-18Co) ($**p < 0.01$ vs. control; $***p < 0.001$ vs. control).

3.2. miR-26a-5p was a target of TUG1 in SW620 cells

The target relationship between TUG1 3′UTR (wt and mut) and miR-26a-5p was predicted by miRDB (http://mirdb.org/) (Fig. 2A). The expression level of miR-26a-5p was monitored by RT-qPCR. As shown in Fig. 2B, the mRNA level of miR-26a-5p was markedly increased in the sh-TUG1 group (Fig. 2B). However, opverexpression of TUG1 significantly decreased miR-26a-5p level (Fig. 2C). Dual luciferase reporter assay showed that luciferase activity was significantly reduced in SW620 cells co-transfected with TUG wt and miR-26a-5p mimic, whereas no significant changes were detected in SW620 cells transfected with TUG wt alone or TUG mut or/and miR-26a-5p mimic (Fig. 2D). In short, these results indicated that miR-26a-5p was a target of TUG1 in SW620 cells.

3.3. TUG1 promoted proliferation and invasion of SW620 cells by regulating miR-26a-5p/MMP-14 axis

The target relationship between miR-26a-5p and MMP-14 3′UTR (wt and mut) was predicted by Targetscan7.0 (http://www.targetscan.org) (Fig. 3A). The expression level of MMP-14 was monitored by western blot. As shown in Fig. 3B, the level of MMP-14 in the sh-TUG1 group was noticeably decreased, indicating that TUG1 and MMP-14 had a positive regulatory relationship. BrdU staining was applied to investigate the proliferative ability, while transwell assay was utilized to determine the invasive capacity. As shown in Fig. 3C, BrdU-positive cells in the sh-TUG1 group were significantly less than the control group. Meanwhile, transwell assay showed that the number of invading cells in the sh-TUG1 group was also significantly reduced. Notably, the miR-26a-3p inhibitor reversed the inhibitory effects of sh-TUG1 on cell proliferation and invasion (Fig. 3D). Taken together, our results indicated that TUG1 promoted proliferation and invasion of SW620 cells by regulating miR-26a-5p/MMP-14 axis.

3.4. TUG1 accelerated the epithelial-mesenchymal transition (EMT) of SW620 cells

Western blotting and immunofluorescent assay were applied to investigate the EMT process of SW620 cells. As shown in Fig. 4A, the downregulation of TUG1 significantly inhibited the expression of mesenchymal marker proteins (Vimentin and N-cadherin) in SW620 cells

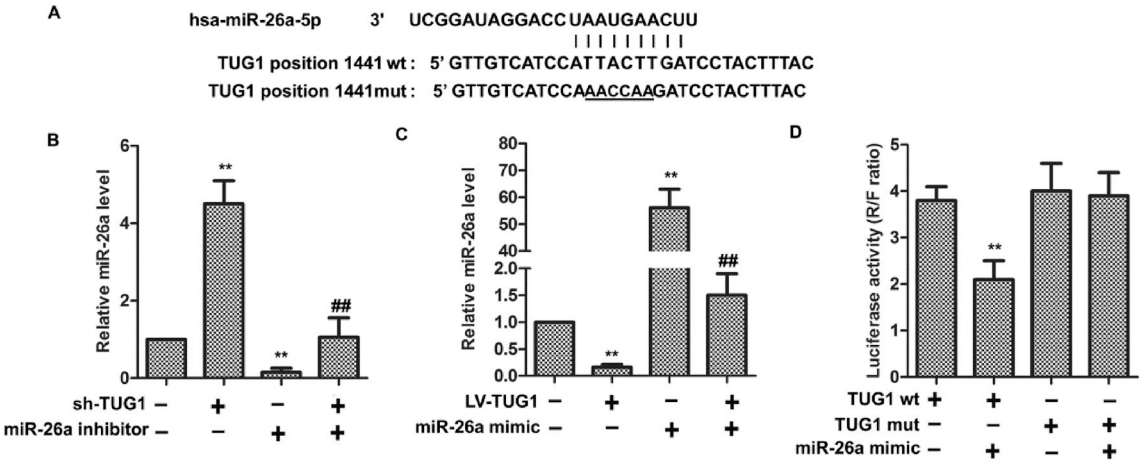

Fig. 2. miR-26a-5p was a target of TUG1 in SW620 cells. A. miR-26a-5p was a target of TUG1. B. miR-26a-5p was measured by RT-qPCR in SW620 cells transfected with sh-TUG1 or/and miR-26a-5p inhibitor (**$p < 0.01$ vs. control; ##$p < 0.01$ vs. miR-26a-5p inhibitor group). C. miR-26a-5p was measured by RT-qPCR in SW620 cells transfected with LV-TUG1 or/and miR-26a-5p mimic (**$p < 0.01$ vs. control, ##$p < 0.01$ vs. miR-22–3p mimic group). D. Luciferase activity of TUG1 was measured in SW620 cells transfected with TUG1 (wt or mut) alone or with miR-26a-5p mimic by dual luciferase reporter assay (**$p < 0.01$ vs. control).

and promoted the expression of epithelial marker protein (E-cadherin). Contrary results were observed in the miR-26a inhibitor group. In addition, immunofluorescent assay showed that sh-TUG1 significantly reduced the number of Vimentin + punctum per cell. However, this effect was counteracted by miR-22–3p inhibitor (Fig. 4B). Therefore, the present study suggested that TUG1 accelerated the EMT process in SW620 cells.

3.5. TUG1 worked in vitro via miR-26a-5p/MMP-14/p38 MAPK/Hsp27 axis

SW620 cells were infected with LV-TUG1 lentivirus or/and treated with SB203580. The levels of MMP-14, VEGF, p-p38 and p-Hsp27 were determined by western blotting. As shown in Fig. 5A, overexpression of TUG1 sigficantly elevated the levels of MMP-14 and VEGF, and accelerated the phosphorylation of p38 (p-p38) and Hsp27 (p-Hsp27). However, the addition of SB203580, a p38 MAPK inhibitor, significantly reduced the levels of MMP-14, VEGF, p-p38 and p-Hsp27 in SW620 cells. Besides, BrdU staining and transwell assay showed that TUG1 overexpression significantly increased the number of BrdU-positive cells and invasive cells, while SB203580 abolished the promotional effect. (Fig. 5B and C). Furthermore, immunofluorescent assay showed that TUG1 overexpression significanly increased the level of vimentin in the nucleus (Fig. 5D), whereas SB203580 abolished the promotional effect. Taken together, these results suggested that TUG1 works *in vitro* via miR-26a-5p/MMP-14/p38 MAPK/Hsp27 axis.

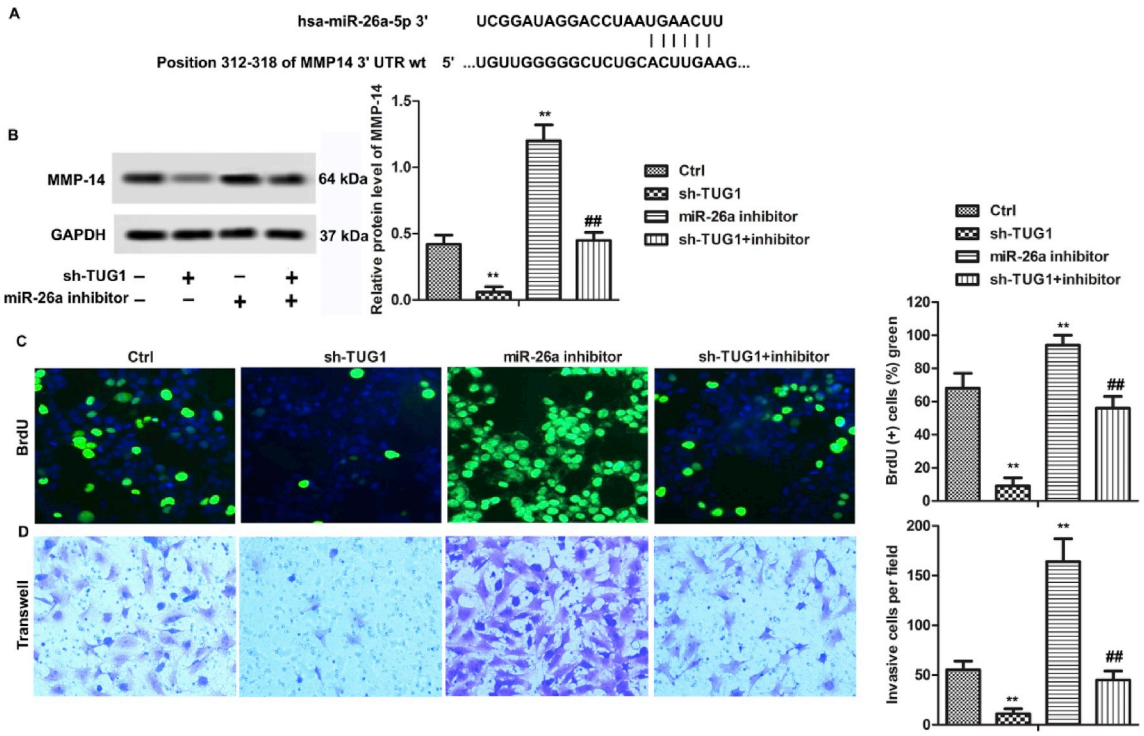

Fig. 3. TUG1 promoted proliferation and invasion of SW620 cells by regulating miR-26a-5p/MMP-14 axis. SW620 cells were transfected with sh-TUG1 or/and miR-26a inhibitor. A. MMP-14 was a target of miR-26a-5p. B. The level of MMP-14 was measured by western blotting. C. Proliferation capacity was measured by BrdU staining. D. Invasive ability was evaluated by transwell assay (**$p < 0.01$ vs. control; ##$p < 0.01$ vs. miR-26a-5p inhibitor group).

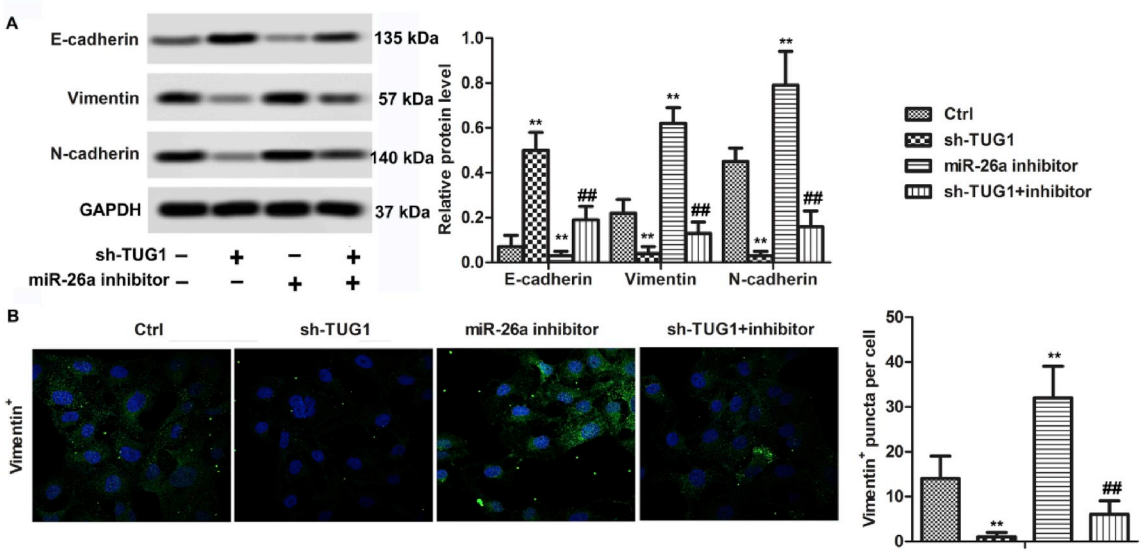

Fig. 4. TUG1 accelerated the epithelial-mesenchymal transition (EMT) of SW620 cells. SW620 cells were transfected with sh-TUG1 or/and miR-26a inhibitor. A. EMT marker protein was monitored by western blotting. B. The level of Vimentin in nucleus was monitored by immunofluorescent assay (**$p < 0.01$ vs. control; ##$p < 0.01$ vs. miR-26a-5p inhibitor group).

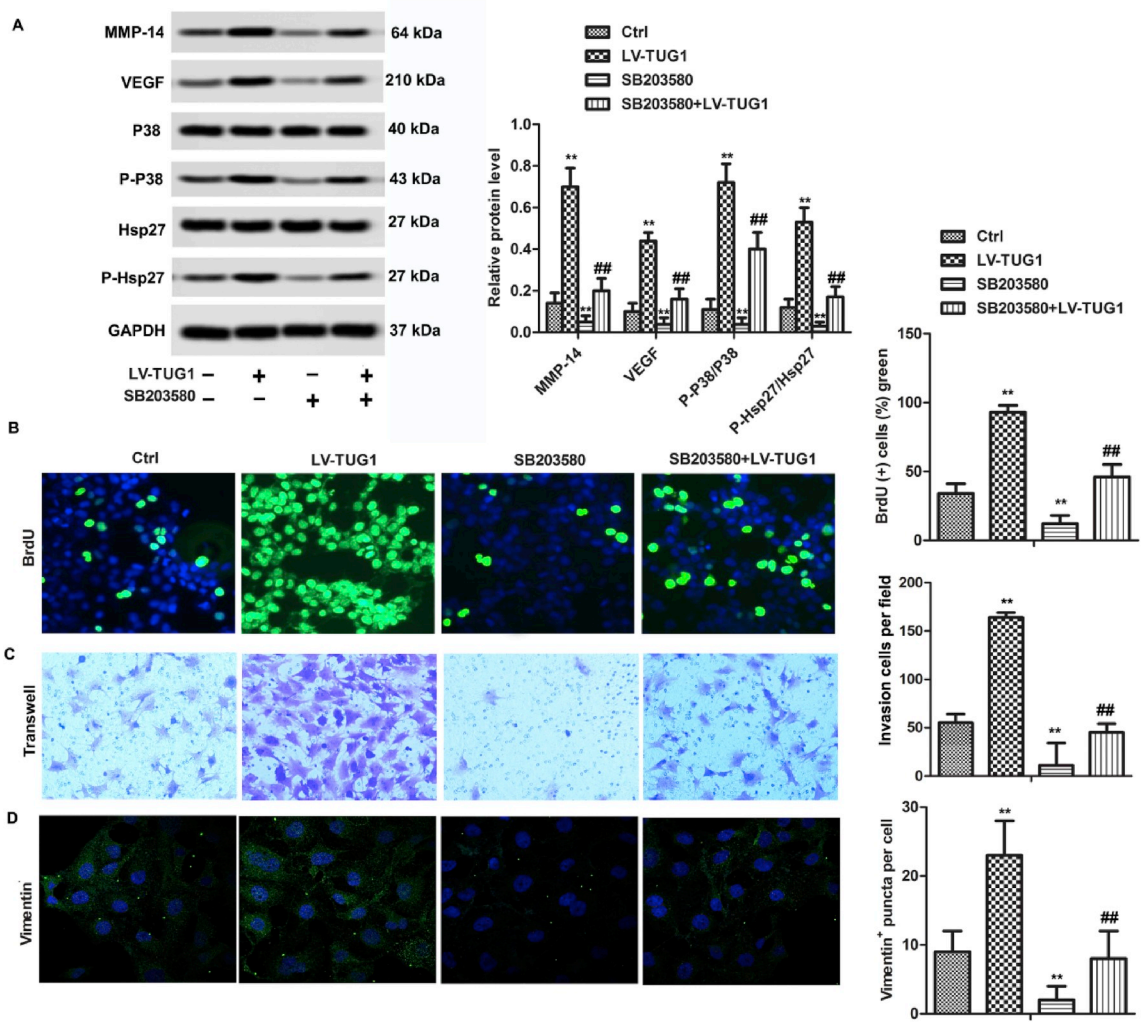

Fig. 5. TUG1 worked *in vivo* via miR-26a-5p/MMP-14/p38 MAPK/Hsp27 axis. SW620 cells were transfected with LV-TUG1 or/and SB203580. A. The levels of MMP-14, VEGF, P38, P–P38, HSP27 and P-HSP27 were measured by western blotting. B. Proliferation capacity was measured by BrdU staining. C. Invasive ability was evaluated by transwell assay. D. The level of Vimentin in nucleus was monitored by immunofluorescent assay (**$p < 0.01$ vs. control; ##$p < 0.01$ vs. SB203580 group).

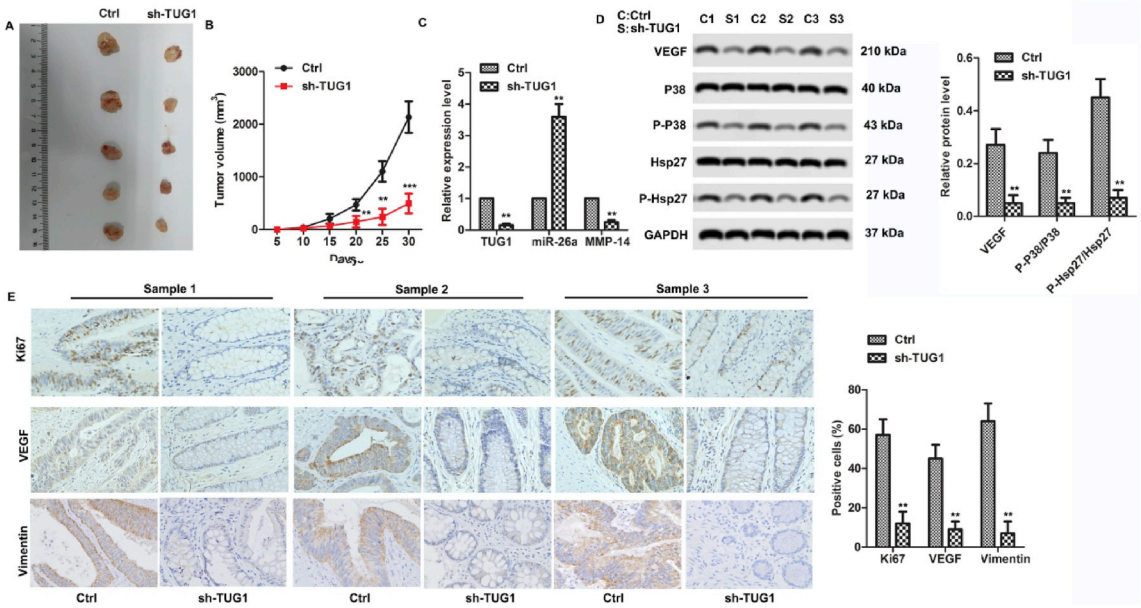

Fig. 6. Low-expression of TUG1 suppressed tumor growth and motility by miR-26a-5p/MMP-14/p38 MAPK/Hsp27 axis *in vivo*. Untreated SW620 cells or SW620 cells transfected with sh-TUG1 were subcutaneously injected into the flank area of mice. Xenograft nude mice were randomly divided into 2 groups with 10 in each group. A. Tumor images. B. Tumor volume. C. The expression level of TUG1, miR-26a and MMP-14 were measured by RT-qPCR. D. The levels of VEGF, p-P-P38 and P-Hsp27 were measured by western blotting. E. The expression of Proliferation marker proteins Ki-67 and VEGF in tumor tissues from xenograft nude mice was measured by IHC. All experiments were conducted in triplicate (**$p < 0.01$ vs. control).

3.6. Low-expression of TUG1 suppressed tumor growth and motility by miR-26a-5p/MMP-14/p38 MAPK/Hsp27 axis in vivo

In this study, mice models were constructed to explore the effect and the potential molecular mechanism of TUG1 on tumors *in vivo*. Untreated SW620 cells or SW620 cells transfected with sh-TUG1 were subcutaneously injected into the flank area of mice. The tumor was taken out and weighed 30 days later. As shown in Fig. 6A and B, the weight and volume of tumor in the sh-TUG1 group were significantly reduced, indicating that tumor growth was significantly inhibited. In addition, RT-qPCR assay showed that a large amount of miR-26a-5p were accumulated in sh-TUG1 group, while the expression of TUG1 and MMP-14 was decreased (Fig. 6C). Western blotting indicated that sh-TUG1 significantly suppressed the expression of VEGF and the phosphorylation of p38 and Hsp27 (Fig. 6D). Furthermore, IHC analysis showed that the levels of Ki-67, VEGF and Vimentin in the tumor tissues of the sh-TUG1 group were significantly reduced (Fig. 6E). Collectively, these findings indicated that low-expression of TUG1 suppressed tumor growth and motility by miR-26a-5p/MMP-14/p38 MAPK/Hsp27 axis *in vivo*.

4. Discussion

Cc is often associated with distant metastasis. Therefore, it is of great significance to in-depth investigate the pathogenesis for the treatment and prevention of *Cc*. This study found that TUG1 and miR-26a-5p were abnormally expressed in cc, suggesting that TUG1 and miR-26a-5p may be closely related to the occurrence of *Cc*.

Abnormally expressed MMP-14 could destroy the inhibitory effect of SDC2-ECD on angiogenesis [9] and induce metastasis of breast cancer [17]. TUG1 plays an important role in cancers. Liu et al. and [30]. found that TUG1 promoted the proliferation and migration in renal cell carcinoma and laryngeal cancer [14,31]. Besides, TUG1 promoted the progression of *Cc* by regulating the Wnt/beta-catenin pathway [23,28]. Consistent with these results, we found that overexpression of TUG1 significantly promoted the proliferation, invasion and EMT of SW620 cells. However, sh-TUG1 significantly abolished the promotional effects *in vivo* and *in vitro*. Further mechanism analysis showed that TUG1 achieved all effects by targeting miR-26a-5p to regulate MMP-14/p38 MAPK/Hsp27 axis.

miR-26a-5p is regulated by multiple lncRNAs and is involved in tumorigenesis. Liang et al. found to promote proliferation, metastasis and EMT of LUAD cells by competitive adsorption of miR-26a-5p [11]. As reported by Yang et al., SNHG5 promoted invasion and migration of HTR-8/SVneo cells by targeting and negatively regulating miR-26a-5p [25]. On this basis, this study found that miR-26a-5p is one of the targets of TUG1, and MMP-14 is the target of miR-26a-5p. Overexpression of TUG1 significantly reduced the level of miR-26a-5p and increased the level of MMP-14, thereby promoting the proliferation and motility of SW620 cells *in vitro*. In addition, overexpression of miR-26a-5p significantly inhibited tumor formation and metastasis in *Cc* mice. Collectively, this study demonstrated that TUG1 regulatestumorigenesis and metastasis via miR-26a-5p/MMP-14 axis *in vitro* and *in vivo*.There is increasing evidence that the p38 MAPK/Hsp27 pathway is associated with various diseases, especially cancers. Zheng et al. reported that knockdown of SPERT by siRNA inhibited proliferation and induced apoptosis of colorectal cancer by regulating the p38 MAPK/Hsp27 pathway [32]. Additionally, Henriques et al. suggested that MK2 promoted tumorigenesis of colorectal cancer by activating the p38 MAPK/Hsp27 pathway [6]. Similarity, the present study showed that LV-TUG1 significantly activated the p38 MAPK/Hsp27 pathway, whereas the p38 MAPK pathway inhibitor reversed the promotional effect of LV-TUG1 on the p38 MAPK/Hsp27 pathway. Taken together, all these results indicate that TUG1 accelerated tumorigenesis and EMT in *Cc* by activating the P38MAPK/Hsp27 pathway *in vivo* and *in vitro*.

In conclusion, this study showed that TUG1 was remarkedly overexpressed in both *Cc* cells and tumors, while sh-TUG1 repressed the growth and motility of *Cc* cells via miR-26a-5p/MMP-14/p38 MAPK/Hsp27 axis *in vivo* and *in vitro*. Therefore, designing targeted drugs for TUG1 provides a new direction for the treatment of *Cc*.

Author contributions

Lei Tian, Zhi-Feng Zhao, Ling Xie and Jin-Peng Zhu conceived and

designed the research; Lei Tian, Zhi-Feng Zhao, Ling Xie and Jin-Peng Zhu performed the experiments; Lei Tian, Zhi-Feng Zhao analyzed the data; Ling Xie established the animal models; Lei Tian, Zhi-Feng Zhao, Ling Xie and Jin-Peng Zhu wrote the manuscript. All authors read the manuscript and approved the final version of the manuscript.

Compliance with ethical standards

Funding: No avaliable.

Ethical approval: This article does not contain any studies with human participants. Animal procedures were approved by the Institutional Animal Care and Use Committee of Jinzhou Medical University.

Declaration of competing interest

The authors declare that there are no conflicts of interest.

Acknowledgement

This study was supported by the Scientific Research Project of Liaoning Provincial Department of Science and Technology (2015020329).

References

[1] B.A. 3Rd, A.P. Venook, L. Cederquist, E. Chan, Y.J. Chen, H.S. Cooper, et al., Colon cancer, version 1.2017, NCCN clinical practice guidelines in oncology, Journal of the National Comprehensive Cancer Network Jnccn 15 (2017) 370.

[2] N.,. Akanuma, I.,. Hoshino, Y.,. Akutsu, K.,. Murakami, Y.,. Isozaki, T.,. Maruyama, et al., MicroRNA-133a regulates the mRNAs of two invadopodia-related proteins, FSCN1 and MMP14, in esophageal cancer, Br. J. Canc. 110 (2014) 189–198.

[3] D. Di, L. Chen, Y. Guo, L. Wang, H. Wang, J. Ju, Association of BCSC-1 and MMP-14 with human breast cancer, Oncology Letters 15 (2018).

[4] O.,. Glehen, F.,. Kwiatkowski, P.H. Sugarbaker, D.,. Elias, E.A. Levine, M. Simone, De, et al., Cytoreductive surgery combined with perioperative intraperitoneal chemotherapy for the management of peritoneal carcinomatosis from colorectal cancer: a multi-institutional study, Journal of Clinical Oncology Official Journal of the American Society of Clinical Oncology 22 (2004) 3284–3292.

[5] He C, Liu Z, Jin L, Zhang F, Peng X, Xiao Y, et al. LncRNA TUG1-Mediated Mir-142-3p Downregulation Contributes to Metastasis and the Epithelial-To-Mesenchymal Transition of Hepatocellular Carcinoma by Targeting ZEB12018.

[6] A. Henriques, V. Koliaraki, G. Kollias, Mesenchymal MAPKAPK2/HSP27 drives intestinal carcinogenesis, Proc. Natl. Acad. Sci. U.S.A. 115 (2018) E5546–E5555.

[7] W. Kun-Peng, L. Qiang, L. Fu-Xiang, L. Jun, W. Lu-Min, L. Wei, et al., MT1-MMP is not a good prognosticator of cancer survival: evidence from 11 studies, Tumour Biology the Journal of the International Society for Oncodevelopmental Biology & Medicine 35 (2014) 12489.

[8] J.M. Kyriakis, J. Avruch, Mammalian mitogen-activated protein kinase signal transduction pathways activated by stress and inflammation, Physiol. Rev. 81 (2001) 807–869.

[9] Y.H. Lee, J.H. Park, D.H. Cheon, T. Kim, Y.E. Park, E.S. Oh, et al., Processing of syndecan-2 by matrix metalloproteinase-14 and effect of its cleavage on VEGF-induced tube formation of HUVECs, Biochem. J. 474 (2017) BCJ20170340.

[10] P. Li, Q. Li, Y. Zhang, S. Sun, S. Liu, Z. Lu, MiR-422a targets MAPKK6 and regulates cell growth and apoptosis in colorectal cancer cells, Biomed. Pharmacother. 104 (2018) S0753332217367811.

[11] R. Liang, G. Xiao, M. Wang, X. Li, Y. Li, Z. Hui, et al., SNHG6 functions as a competing endogenous RNA to regulate E2F7 expression by sponging miR-26a-5p in lung adenocarcinoma, Biomed. Pharmacother. 107 (2018) 1434–1446.

[12] T. Liao, N. Qu, R.L. Shi, K. Guo, B. Ma, Y.M. Cao, J. Xiang, Z.W. Lu, Y.X. Zhu, D.S. Li, BRAF-activated LncRNA functions as a tumor suppressor in papillary thyroid cancer, Oncotarget 2016 8 (2016) 238–247.

[13] C.Z. Lin, R.W. Ou, Y.H. Hu, Lentiviral-mediated microRNA-26b up-regulation inhibits proliferation and migration of hepatocellular carcinoma cells, Kaohsiung J. Med. Sci. (2018) S1607551X17308847-.

[14] S. Liu, Y. Yang, W. Wang, X. Pan, Long noncoding RNA TUG1 promotes cell proliferation and migration of renal cell carcinoma via regulation of YAP, J. Cell. Biochem. 119 (2018) 9694–9706.

[15] M. Mirakhorli, S.A. Rahman, S. Abdullah, M. Vakili, R. Rozafzon, A. Khoshzaban, Multidrug resistance protein 2 genetic polymorphism and colorectal cancer recurrence in patients receiving adjuvant FOLFOX-4 chemotherapy, Mol. Med. Rep. 7 (2013) 613–617.

[16] K. Miyamoto, N. Seki, R. Matsushita, M. Yonemori, H. Yoshino, M. Nakagawa, et al., Tumour-suppressivemiRNA-26a-5pandmiR-26b-5pinhibit cell aggressiveness by regulatingPLOD2in bladder cancer, Br. J. Canc. 115 (2016) 354–363.

[17] E. Mylona, A. Nomikos, C. Magkou, M. Kamberou, I. Papassideri, A. Keramopoulos, et al., The clinicopathological and prognostic significance of membrane type 1 matrix metalloproteinase (MT1-MMP) and MMP-9 according to their localization in invasive breast carcinoma, Histopathology 50 (2007) 338–347.

[18] S. Rebecca, M. Jiemin, Z. Zhaohui, J. Ahmedin, Cancer Statistics, Ca A Cancer Journal for Clinicians, 2014 2013.

[19] Rui L, Guodong X, Meng W, Xiang L, Yuan L, Zengqian H, et al. SNHG6 functions as a competing endogenous RNA to regulate E2F7 expression by sponging miR-26a-5p in lung adenocarcinoma. Biomed. Pharmacother..107:1434-1446.

[20] L.A. Torre, B. Freddie, R.L. Siegel, F. Jacques, L.T. Joannie, J. Ahmedin, Global cancer statistics, Ca - Cancer J. Clin. 65 (2012) 87–108 2015.

[21] H. Wang, Z. Hu, L. Chen, Enhanced plasma miR-26a-5p promotes the progression of bladder cancer via targeting PTEN, Oncol Lett 16 (2018) 4223–4228.

[22] Y. Wang, S. Guan, G. Zhao, P. Shi, J. Wang, [Expressions of aquaporin-4, matrix metallo-proteinase-2 and matrix metallo-proteinase-14 in peritumor edematous zone of glioma and clinical implications], Zhonghua Yixue Zazhi 94 (2014) 2290–2292.

[23] C.H. Xiao, H.Z. Yu, C.Y. Guo, Z.M. Wu, H.Y. Cao, W.B. Li, et al., Long non-coding RNA TUG1 promotes the proliferation of colorectal cancer cells through regulating Wnt/β-catenin pathway, Oncology Letters 16 (2018) 5317–5324.

[24] W. Xu, L. He, Y. Li, Y. Tan, F. Zhang, H. Xu, Silencing of lncRNA ZFAS1 inhibits malignancies by blocking Wnt/β-catenin signaling in gastric cancer cells, Biosci. Biotechnol. Biochem. 82 (2018) 1.

[25] Y. Yang, L. Xi, Y. Ma, X. Zhu, R. Chen, L. Luan, et al., The lncRNA small nucleolar RNA host gene 5 regulates trophoblast cell proliferation, invasion, and migration via modulating miR-26a-5p/N-cadherin axis, J. Cell. Biochem. (2018).

[26] T.L. Young, T.,. Matsuda, C.L. Cepko, The noncoding RNA taurine upregulated gene 1 is required for differentiation of the murine retina, Current Biology Cb 15 (2005) 501–512.

[27] H. Yuan, W. Ran, Y. Xiao, S. Yi, W. Jia, H. Yu, et al., RHBDF1 regulates APC-mediated stimulation of the epithelial-to-mesenchymal transition and proliferation of colorectal cancer cells in part via the Wnt/β-catenin signalling pathway, Exp. Cell Res. 368 (2018).

[28] H.-Y. Zhai, M.-H. Sui, X. Yu, Z. Qu, J.-C. Hu, H.-Q. Sun, et al., Overexpression of long non-coding RNA TUG1 promotes colon cancer progression, Med. Sci. Monit.: International Medical Journal Of Experimental And Clinical Research 22 (2016) 3281–3287.

[29] H.Y. Zhai, M.H. Sui, Y. Xiao, Q. Zhen, J.C. Hu, H.Q. Sun, et al., Overexpression of long non-coding RNA TUG1 promotes colon cancer progression, Medical Science Monitor International Medical Journal of Experimental & Clinical Research 22 (2016) 3281–3287.

[30] Zhang Z, Wang X, Cao S, Han X, Wang Z, Zhao X, et al. The long noncoding RNA TUG1 promotes laryngeal cancer proliferation and migration. Cell. Physiol. Biochem..

[31] Z. Zhang, X. Wang, S. Cao, X. Han, Z. Wang, X. Zhao, et al., The long noncoding RNA TUG1 promotes laryngeal cancer proliferation and migration, Cell. Physiol. Biochem.: International Journal Of Experimental Cellular Physiology, Biochemistry, And Pharmacology 49 (2018) 2511–2520.

[32] L.-Z. Zheng, S.-Z. Chen, shRNA-induced knockdown of the SPERT gene inhibits proliferation and promotes apoptosis of human colorectal cancer RKO cells, Oncol. Rep. 40 (2018) 813–822.